

# Improved Constraints on $D^0\text{-}\bar{D}^0$ Mixing in $D^0 \rightarrow K^+\pi^-$ Decays from the Belle Detector

L. M. Zhang,<sup>35</sup> Z. P. Zhang,<sup>35</sup> J. Li,<sup>35</sup> K. Abe,<sup>7</sup> K. Abe,<sup>42</sup> I. Adachi,<sup>7</sup> H. Aihara,<sup>44</sup> D. Anipko,<sup>1</sup> K. Arinstein,<sup>1</sup> Y. Asano,<sup>48</sup> T. Aushev,<sup>11</sup> S. Bahinipati,<sup>4</sup> A. M. Bakich,<sup>39</sup> V. Balagura,<sup>11</sup> M. Barbero,<sup>6</sup> A. Bay,<sup>16</sup> I. Bedny,<sup>1</sup> K. Belous,<sup>10</sup> U. Bitenc,<sup>12</sup> I. Bizjak,<sup>12</sup> S. Blyth,<sup>22</sup> A. Bondar,<sup>1</sup> A. Bozek,<sup>25</sup> M. Bračko,<sup>7,18,12</sup> J. Brodzicka,<sup>25</sup> T. E. Browder,<sup>6</sup> M.-C. Chang,<sup>43</sup> P. Chang,<sup>24</sup> Y. Chao,<sup>24</sup> A. Chen,<sup>22</sup> W. T. Chen,<sup>22</sup> B. G. Cheon,<sup>3</sup> R. Chistov,<sup>11</sup> S.-K. Choi,<sup>5</sup> Y. Choi,<sup>38</sup> Y. K. Choi,<sup>38</sup> A. Chuvikov,<sup>32</sup> S. Cole,<sup>39</sup> J. Dalseno,<sup>19</sup> M. Danilov,<sup>11</sup> M. Dash,<sup>49</sup> A. Drutskoy,<sup>4</sup> S. Eidelman,<sup>1</sup> N. Gabyshev,<sup>1</sup> T. Gershon,<sup>7</sup> A. Go,<sup>22</sup> G. Gokhroo,<sup>40</sup> B. Golob,<sup>17,12</sup> A. Gorišek,<sup>12</sup> H. C. Ha,<sup>14</sup> J. Haba,<sup>7</sup> T. Hara,<sup>29</sup> N. C. Hastings,<sup>44</sup> K. Hayasaka,<sup>20</sup> H. Hayashii,<sup>21</sup> M. Hazumi,<sup>7</sup> Y. Hoshi,<sup>42</sup> S. Hou,<sup>22</sup> W.-S. Hou,<sup>24</sup> Y. B. Hsiung,<sup>24</sup> T. Iijima,<sup>20</sup> K. Ikado,<sup>20</sup> K. Inami,<sup>20</sup> A. Ishikawa,<sup>7</sup> H. Ishino,<sup>45</sup> R. Itoh,<sup>7</sup> M. Iwasaki,<sup>44</sup> Y. Iwasaki,<sup>7</sup> J. H. Kang,<sup>50</sup> P. Kapusta,<sup>25</sup> N. Katayama,<sup>7</sup> H. Kawai,<sup>2</sup> T. Kawasaki,<sup>26</sup> H. Kichimi,<sup>7</sup> H. J. Kim,<sup>15</sup> S. K. Kim,<sup>36</sup> S. M. Kim,<sup>38</sup> K. Kinoshita,<sup>4</sup> S. Korpar,<sup>18,12</sup> P. Križan,<sup>17,12</sup> P. Krokovny,<sup>1</sup> R. Kulasiri,<sup>4</sup> R. Kumar,<sup>30</sup> C. C. Kuo,<sup>22</sup> A. Kuzmin,<sup>1</sup> Y.-J. Kwon,<sup>50</sup> G. Leder,<sup>9</sup> J. Lee,<sup>36</sup> T. Lesiak,<sup>25</sup> S.-W. Lin,<sup>24</sup> D. Liventsev,<sup>11</sup> F. Mandl,<sup>9</sup> T. Matsumoto,<sup>46</sup> Y. Mikami,<sup>43</sup> W. Mitaroff,<sup>9</sup> K. Miyabayashi,<sup>21</sup> H. Miyake,<sup>29</sup> H. Miyata,<sup>26</sup> Y. Miyazaki,<sup>20</sup> R. Mizuk,<sup>11</sup> D. Mohapatra,<sup>49</sup> T. Mori,<sup>45</sup> M. Nakao,<sup>7</sup> Z. Natkaniec,<sup>25</sup> S. Nishida,<sup>7</sup> O. Nitoh,<sup>47</sup> T. Nozaki,<sup>7</sup> S. Ogawa,<sup>41</sup> T. Ohshima,<sup>20</sup> T. Okabe,<sup>20</sup> S. Okuno,<sup>13</sup> S. L. Olsen,<sup>6</sup> W. Ostrowicz,<sup>25</sup> H. Ozaki,<sup>7</sup> C. W. Park,<sup>38</sup> H. Park,<sup>15</sup> R. Pestotnik,<sup>12</sup> L. E. Piilonen,<sup>49</sup> Y. Sakai,<sup>7</sup> N. Sato,<sup>20</sup> N. Satoyama,<sup>37</sup> T. Schietinger,<sup>16</sup> O. Schneider,<sup>16</sup> C. Schwanda,<sup>9</sup> A. J. Schwartz,<sup>4</sup> R. Seidl,<sup>33</sup> K. Senyo,<sup>20</sup> M. E. Sevier,<sup>19</sup> M. Shapkin,<sup>10</sup> H. Shibuya,<sup>41</sup> B. Shwartz,<sup>1</sup> J. B. Singh,<sup>30</sup> A. Sokolov,<sup>10</sup> A. Somov,<sup>4</sup> N. Soni,<sup>30</sup> R. Stamen,<sup>7</sup> S. Stanič,<sup>27</sup> M. Starič,<sup>12</sup> K. Sumisawa,<sup>29</sup> T. Sumiyoshi,<sup>46</sup> S. Suzuki,<sup>34</sup> F. Takasaki,<sup>7</sup> K. Tamai,<sup>7</sup> N. Tamura,<sup>26</sup> M. Tanaka,<sup>7</sup> G. N. Taylor,<sup>19</sup> Y. Teramoto,<sup>28</sup> X. C. Tian,<sup>31</sup> K. Trabelsi,<sup>6</sup> T. Tsuboyama,<sup>7</sup> T. Tsukamoto,<sup>7</sup> S. Uehara,<sup>7</sup> T. Uglov,<sup>11</sup> K. Ueno,<sup>24</sup> Y. Unno,<sup>7</sup> S. Uno,<sup>7</sup> P. Urquijo,<sup>19</sup> Y. Usov,<sup>1</sup> G. Varner,<sup>6</sup> S. Villa,<sup>16</sup> C. C. Wang,<sup>24</sup> C. H. Wang,<sup>23</sup> Y. Watanabe,<sup>45</sup> E. Won,<sup>14</sup> Q. L. Xie,<sup>8</sup> B. D. Yabsley,<sup>39</sup> A. Yamaguchi,<sup>43</sup> M. Yamauchi,<sup>7</sup> J. Ying,<sup>31</sup> Y. Yuan,<sup>8</sup> C. C. Zhang,<sup>8</sup> J. Zhang,<sup>7</sup> V. Zhilich,<sup>1</sup> and D. Zürcher<sup>16</sup>

(The Belle Collaboration)

<sup>1</sup>*Budker Institute of Nuclear Physics, Novosibirsk*

<sup>2</sup>*Chiba University, Chiba*

<sup>3</sup>*Chonnam National University, Kwangju*

<sup>4</sup>*University of Cincinnati, Cincinnati, Ohio 45221*

<sup>5</sup>*Gyeongsang National University, Chinju*

<sup>6</sup>*University of Hawaii, Honolulu, Hawaii 96822*

<sup>7</sup>*High Energy Accelerator Research Organization (KEK), Tsukuba*

<sup>8</sup>*Institute of High Energy Physics, Chinese Academy of Sciences, Beijing*

<sup>9</sup>*Institute of High Energy Physics, Vienna*

<sup>10</sup>*Institute of High Energy Physics, Protvino*

<sup>11</sup>*Institute for Theoretical and Experimental Physics, Moscow*

<sup>12</sup>*J. Stefan Institute, Ljubljana*

<sup>13</sup>*Kanagawa University, Yokohama*

<sup>14</sup>*Korea University, Seoul*

<sup>15</sup>*Kyungpook National University, Taegu*

<sup>16</sup>*Swiss Federal Institute of Technology of Lausanne, EPFL, Lausanne*

<sup>17</sup>*University of Ljubljana, Ljubljana*

<sup>18</sup>*University of Maribor, Maribor*

<sup>19</sup>*University of Melbourne, Victoria*

<sup>20</sup>*Nagoya University, Nagoya*

<sup>21</sup>*Nara Women's University, Nara*

<sup>22</sup>*National Central University, Chung-li*

<sup>23</sup>*National United University, Miao Li*

<sup>24</sup>*Department of Physics, National Taiwan University, Taipei*

<sup>25</sup>*H. Niewodniczanski Institute of Nuclear Physics, Krakow*

<sup>26</sup>*Niigata University, Niigata*

<sup>27</sup>*Nova Gorica Polytechnic, Nova Gorica*

<sup>28</sup>*Osaka City University, Osaka*

<sup>29</sup>*Osaka University, Osaka*

<sup>30</sup>*Panjab University, Chandigarh*

<sup>31</sup>*Peking University, Beijing*

<sup>32</sup>Princeton University, Princeton, New Jersey 08544

<sup>33</sup>RIKEN BNL Research Center, Upton, New York 11973

<sup>34</sup>Saga University, Saga

<sup>35</sup>University of Science and Technology of China, Hefei

<sup>36</sup>Seoul National University, Seoul

<sup>37</sup>Shinshu University, Nagano

<sup>38</sup>Sungkyunkwan University, Suwon

<sup>39</sup>University of Sydney, Sydney NSW

<sup>40</sup>Tata Institute of Fundamental Research, Bombay

<sup>41</sup>Toho University, Funabashi

<sup>42</sup>Tohoku Gakuin University, Tagajo

<sup>43</sup>Tohoku University, Sendai

<sup>44</sup>Department of Physics, University of Tokyo, Tokyo

<sup>45</sup>Tokyo Institute of Technology, Tokyo

<sup>46</sup>Tokyo Metropolitan University, Tokyo

<sup>47</sup>Tokyo University of Agriculture and Technology, Tokyo

<sup>48</sup>University of Tsukuba, Tsukuba

<sup>49</sup>Virginia Polytechnic Institute and State University, Blacksburg, Virginia 24061

<sup>50</sup>Yonsei University, Seoul

We report the results of a search for  $D^0$ - $\bar{D}^0$  mixing in  $D^0 \rightarrow K^+\pi^-$  decays based on 400 fb<sup>-1</sup> of data accumulated by the Belle detector at KEKB. Both assuming  $CP$  conservation and allowing for  $CP$  violation, we fit the decay-time distribution for the mixing parameters  $x'$  and  $y'$ , as well as for the parameter  $R_D$ , the ratio of doubly-Cabibbo-suppressed decays to Cabibbo-favored decays. The 95% confidence level region in the  $(x'^2, y')$  plane is obtained using a frequentist method. Assuming  $CP$  conservation, we find  $x'^2 < 0.72 \times 10^{-3}$  and  $-9.9 \times 10^{-3} < y' < 6.8 \times 10^{-3}$  at the 95% confidence level; these are the most stringent constraints on the mixing parameters to date. The no-mixing point (0, 0) has a confidence level of 3.9%. Assuming no mixing, we measure  $R_D = (0.377 \pm 0.008 \pm 0.005)\%$ .

PACS numbers: 13.25.Ft, 11.30.Er, 12.15.Ff

The phenomenon of mixing has been observed in the  $K^0$ - $\bar{K}^0$  and  $B^0$ - $\bar{B}^0$  systems, but not yet in the  $D^0$ - $\bar{D}^0$  system. The parameters used to characterize mixing are  $x \equiv \Delta m/\bar{\Gamma}$  and  $y \equiv \Delta\Gamma/(2\bar{\Gamma})$ , where  $\Delta m$  and  $\Delta\Gamma$  are the differences in mass and decay width between the two neutral  $D$  mass eigenstates, and  $\bar{\Gamma}$  is the average width. The mixing rate within the Standard Model is expected to be small [1]. The largest predicted values, including long-distance effects, are of order  $|x| \lesssim |y| \sim (10^{-3} - 10^{-2})$ , and are reachable with the current experimental sensitivity. Observation of  $|x| \gg |y|$  or  $CP$  violation ( $CPV$ ) in  $D^0$ - $\bar{D}^0$  mixing would constitute unambiguous evidence for new physics.

The “wrong-sign” (WS) process,  $D^0 \rightarrow K^+\pi^-$ , can proceed either through direct doubly-Cabibbo-suppressed (DCS) decay or through mixing followed by the “right-sign” (RS) Cabibbo-favored (CF) decay  $D^0 \rightarrow \bar{D}^0 \rightarrow K^+\pi^-$  [2]. The two decays can be distinguished by the decay-time distribution. For  $|x|, |y| \ll 1$ , and assuming negligible  $CPV$ , the decay-time distribution for  $D^0 \rightarrow K^+\pi^-$  can be expressed as

$$\frac{dN}{dt} \propto e^{-\bar{\Gamma}t} \left[ R_D + \sqrt{R_D} y' (\bar{\Gamma}t) + \frac{x'^2 + y'^2}{4} (\bar{\Gamma}t)^2 \right], \quad (1)$$

where  $R_D$  is the ratio of DCS to CF decay rates,  $x' = x \cos \delta + y \sin \delta$ ,  $y' = y \cos \delta - x \sin \delta$ , and  $\delta$  is the strong phase difference between the DCS and CF amplitudes. The first (last) term in brackets is due to the DCS (CF)

amplitude, and the middle term is due to interference between the two processes. The time-integrated rate ( $R_{WS}$ ) for  $D^0 \rightarrow K^+\pi^-$  relative to that for  $D^0 \rightarrow K^-\pi^+$  is  $R_D + \sqrt{R_D} y' + (x'^2 + y'^2)/2$ .

To allow for  $CPV$ , we apply Eq. (1) to  $D^0$  and  $\bar{D}^0$  separately. This results in six observables:  $\{R_D^+, x'^{+2}, y'^{+2}\}$  for  $D^0$  and  $\{R_D^-, x'^{-2}, y'^{-2}\}$  for  $\bar{D}^0$ .  $CPV$  is parameterized by the asymmetries  $A_D = (R_D^+ - R_D^-)/(R_D^+ + R_D^-)$  and  $A_M = (R_M^+ - R_M^-)/(R_M^+ + R_M^-)$ , where  $R_M^\pm = (x'^{\pm 2} + y'^{\pm 2})/2$ .  $A_D$  and  $A_M$  characterize  $CPV$  in DCS decays and in mixing, respectively. The observables are related to  $x'$  and  $y'$  via

$$x'^{\pm} = \left[ \frac{1 \pm A_M}{1 \mp A_M} \right]^{1/4} (x' \cos \phi \pm y' \sin \phi) \quad (2)$$

$$y'^{\pm} = \left[ \frac{1 \pm A_M}{1 \mp A_M} \right]^{1/4} (y' \cos \phi \mp x' \sin \phi), \quad (3)$$

where  $\phi$  is a weak phase and characterizes  $CPV$  occurring in interference between mixed and unmixed decay amplitudes. To avoid ambiguity, we restrict  $\phi$  to the range  $|\phi| < \pi/2$ .

This method has been exploited in previous studies [3, 4, 5, 6, 7]. In our previous measurement based on a 90 fb<sup>-1</sup> data sample, the value of  $y'$  was found to be slightly positive although compatible with zero [6]. Here we exploit the much larger data set now available to search for  $D^0$ - $\bar{D}^0$  mixing with significantly higher sensitivity.

In this Letter we present improved results of an analysis of  $400 \text{ fb}^{-1}$  of data, setting more stringent limits on mixing and  $CPV$  parameters. The data were recorded by the Belle detector at the KEKB asymmetric-energy  $e^+e^-$  collider [8]. The Belle detector [9] includes a silicon vertex detector (SVD), a central drift chamber (CDC), an array of aerogel threshold Cherenkov counters (ACC), a barrel-like arrangement of time-of-flight scintillation counters (TOF), and an electromagnetic calorimeter. The first  $157 \text{ fb}^{-1}$  of data were taken with a 2.0 cm radius beampipe and a 3-layer SVD, while the subsequent  $243 \text{ fb}^{-1}$  were collected with a 1.5 cm radius beampipe, a 4-layer SVD, and a small-cell inner drift chamber [10].

We reconstruct  $D^0$  candidates from the decay chain  $D^{*+} \rightarrow \pi_s^+ D^0$ ,  $D^0 \rightarrow K^\pm \pi^\mp$ . Here,  $\pi_s$  denotes the low-momentum (slow) pion, the charge of which tags the flavor of the neutral  $D$  at production. We select  $D^0$  candidates by requiring two oppositely-charged tracks, each with at least two SVD hits in both  $r$ - $\phi$  and  $z$  coordinate, satisfying  $K$  and  $\pi$  identification selection criteria. These criteria are  $\mathcal{L} > 0.5$  for  $K$  and  $\mathcal{L} < 0.9$  for  $\pi$ , where  $\mathcal{L}$  is the relative likelihood for a track to be a  $K$  based on the response of the ACC and measurements from the CDC and TOF. These criteria have efficiencies of 90% and 94%, and  $\pi/K$  misidentification rates of 10% and 17%, respectively. To reject background candidates in which the  $K$  is misidentified as  $\pi$  and the  $\pi$  is misidentified as  $K$ , we recalculate  $m_{K\pi}$  with the  $K$  and  $\pi$  assignments swapped and reject events with  $|m_{K\pi}^{(\text{swapped})} - m_{D^0}| < 28 \text{ MeV}/c^2$  ( $\sim 4.5\sigma$ ). A  $D^{*+}$  candidate is reconstructed by combining a  $D^0$  candidate with a  $\pi_s$  candidate; the resulting  $D^{*+}$  momentum in the  $e^+e^-$  center-of-mass frame ( $p_{D^*}$ ) is required to be  $> 2.7 \text{ GeV}/c$  in order to eliminate  $B\bar{B}$  events and suppress the combinatorial background.

The  $D^0$  vertex is obtained by fitting its daughter tracks. The  $D^*$  vertex is taken as the intersection of the  $D^0$  trajectory with the interaction region. We constrain  $\pi_s$  to originate from the obtained  $D^*$  vertex. A good  $\chi^2$  for each vertex fit is required. The  $D^0$  proper decay time  $t$  is then calculated. We require the uncertainty of the decay-time  $\sigma_t$  to be less than 0.7 ps (typically,  $\sigma_t \sim 0.13 \text{ ps}$ ).

The selection criteria for particle identification, the  $\chi^2$  of vertex fits, and  $p_{D^*}$  are obtained by maximizing  $N_{\text{sig}}/\sqrt{N_{\text{sig}} + N_{\text{bkg}}}$ , where  $N_{\text{sig}}$  ( $N_{\text{bkg}}$ ) is the expected number of WS signal (background) events estimated from data in the RS signal (WS sideband) region. We assume  $R_{\text{WS}} = 0.37\%$  [6] in the calculation. The optimized values of the selection criteria are similar to those used previously [6].

We select events satisfying  $1.81 \text{ GeV}/c^2 < m_{K\pi} < 1.91 \text{ GeV}/c^2$  and  $0 < Q < 20 \text{ MeV}$ , where  $Q \equiv m_{K\pi\pi_s} - m_{K\pi} - m_\pi$  is the kinetic energy released in the decay. About 5% of selected events have two or more  $D^*$  candidates associated with a single  $D^0$  candidate. If these  $D^*$  candidates have opposite sign, the event is rejected;

this reduces random  $\pi_s$  background (see below) by 30% while reducing the signal by only 1%. If the  $D^*$  candidates have the same sign, then we choose the candidate that has the best  $\chi^2$  resulting from the vertex fit.

We determine RS and WS event yields from a two-dimensional fit to the  $m_{K\pi}$ - $Q$  distribution. There are four significant background sources in the WS sample: (a) random  $\pi_s$  background, in which a random  $\pi^+$  is combined with a  $\bar{D}^0 \rightarrow K^+\pi^-$  decay; (b)  $D^{*+} \rightarrow D^0\pi^+$  followed by  $D^0$  decaying to  $\geq 3$ -body final states; (c)  $D_{(s)}^+$  decays; and (d) combinatorial. They are denoted as rnd, d3b, ds3 and cmb in turn. These background shapes are obtained from Monte Carlo (MC) simulation and fixed in the fit. When fitting the RS sample, the parameters for the signal shape are floated; when fitting the WS sample, these parameters are fixed to the values obtained from the RS fit. We find  $1073993 \pm 1108$  RS and  $4024 \pm 88$  WS signal events, and the ratio of WS to RS events is  $(0.375 \pm 0.008)\%$  (statistical error only). The ratio of WS signal to background is 1.1, about 20% higher than that of our previous study [6]. The background is composed mostly of random  $\pi_s$  (51%) and combinatorial (35%) events. Figure 1 shows the  $m_{K\pi}$  and  $Q$  distributions superimposed with projections of the fit result. The WS projections for  $m_{K\pi}$  and  $Q$  are shown for a  $3\sigma$  signal interval in  $Q$  and  $m_{K\pi}$ , respectively. The contribution of  $D_{(s)}^+$  decays is too small to be seen.

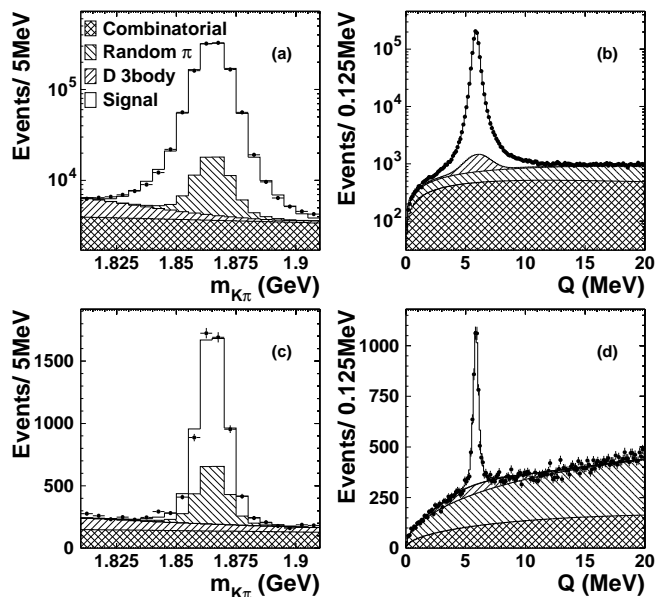


FIG. 1: The distribution for (a) RS  $m_{K\pi}$  with  $0 < Q < 20 \text{ MeV}$ ; (b) RS  $Q$  with  $1.81 \text{ GeV}/c^2 < m_{K\pi} < 1.91 \text{ GeV}/c^2$ ; (c) WS  $m_{K\pi}$  with  $5.3 \text{ MeV} < Q < 6.5 \text{ MeV}$ ; and (d) WS  $Q$  with  $1.845 \text{ GeV}/c^2 < m_{K\pi} < 1.885 \text{ GeV}/c^2$ . Superimposed on the data (points with error bars) are projections of the  $m_{K\pi}$ - $Q$  fit.

The decay-time fitting procedure is similar to that of our previous measurement [6] but with several improve-

ments as discussed below. We determine  $R_D$ ,  $x'^2$  and  $y'$  by applying an unbinned maximum likelihood fit to the distribution of WS proper decay time, considering the  $4\sigma$  region  $|m_{K\pi} - m_{D^0}| < 22 \text{ MeV}/c^2$  and  $|Q - 5.9 \text{ MeV}| < 1.5 \text{ MeV}$ . We determine background shapes by fitting events in an  $m_{K\pi}$  sideband (this contains no signal or random  $\pi_s$  events). The probability density function (PDF) for the WS signal is given by Eq. (1), denoted as  $P_{\text{sig}}$ , convolved with a resolution function  $R_{\text{sig}}(t)$ . The latter is represented by a sum of three Gaussians with widths  $\sigma_j = S_j \cdot \sigma_t$  ( $j = 1 - 3$ ) and a common mean (the error  $\sigma_t$  varies event-by-event). The decay-time distributions for the backgrounds from random  $\pi_s$ , 3-body and  $D_{(s)}^+$  decays are exponential,  $P_k = e^{-t/\tau_k}$  ( $k=\text{rnd}$ ,  $\text{d3b}$ ,  $\text{ds3}$ ), while the distribution of combinatorial background is taken to be a Dirac delta function  $\delta(t)$ . The distributions are also convolved with the corresponding resolution functions  $R_k$  ( $k=\text{d3b}$ ,  $\text{ds3}$ ,  $\text{cmb}$ ) which depend on  $\sigma_t$ . For the main background contribution of random  $\pi_s$ , the resolution function and the lifetime are the same as those of the signal, since the  $\pi_s$  does not affect the  $D^0$  vertex reconstruction. We define a likelihood value for each ( $i$ th) event as a function of  $R_D$ ,  $x'^2$  and  $y'$ :

$$P_i = \int_0^\infty dt' [\{f_{\text{sig}}^i P_{\text{sig}}(t'; R_D, x'^2, y') + f_{\text{rnd}}^i P_{\text{rnd}}(t')\} R_{\text{sig}}(t_i - t') + f_{\text{d3b}}^i P_{\text{d3b}}(t') R_{\text{d3b}}(t_i - t') + f_{\text{ds3}}^i P_{\text{ds3}}(t') R_{\text{ds3}}(t_i - t') + f_{\text{cmb}}^i \delta(t') R_{\text{cmb}}(t_i - t')]. \quad (4)$$

Here, the fractions  $f_k^i$  ( $k = \text{sig}$ ,  $\text{rnd}$ ,  $\text{d3b}$ ,  $\text{ds3}$  or  $\text{cmb}$ ) are determined on an event-by-event basis as functions of  $m_{K\pi}$ ,  $Q$  and  $\sigma_t$ .

The fitting procedure is implemented in steps as follows. First we fit the RS sideband region using a simple background model to obtain parameters of  $R_{\text{d3b}}$ . Then we fit the same events using a full background model as in Eq. (4), which yields  $R_{\text{cmb}}$  and  $\tau_{\text{d3b}}$  for RS background. We fit the RS signal region with these background parameters fixed, and obtain parameters of  $R_{\text{sig}}$  (the scaling factors  $S_j$ , and the mean value and fractions of the individual Gaussians) and the  $D^0$  lifetime  $\tau_{D^0}$ . The latter is found to be  $409.9 \pm 0.7 \text{ fs}$ , in good agreement with the world average value [11]. The  $\chi^2$  of the fit projection on the decay-time distribution is 64.0 for 60 bins. We use different resolution parameters for the two SVD configurations. We then fit the WS sample. We fit the WS sideband region with  $R_{\text{d3b}}$  fixed from the RS sideband fit and the  $D_{(s)}^+$  contribution fixed from MC calculations; this yields  $R_{\text{cmb}}$  and  $\tau_{\text{d3b}}$  for WS background. Finally, we fit to the WS signal region with these background parameters,  $R_{\text{sig}}$  and  $\tau_{D^0}$  fixed. In the final fit,  $R_D$ ,  $x'^2$  and  $y'$  are the only free parameters and are determined by maximizing the extended log-likelihood function  $\ln \mathcal{L} = \sum_i \ln P_i + \ln \mathcal{L}_R$ . The function  $\mathcal{L}_R$  is a Gaussian that constrains the ratio  $R_{\text{WS}}(R_D, x'^2, y')$  to

be near the value obtained from the  $m_{K\pi}$ - $Q$  fit; this is needed because  $P_{\text{sig}}(t'; R_D, x'^2, y')$  is normalized to unity.

The main improvements in the decay-time fitting procedure with respect to that of our previous measurements on a smaller data set [6] consist of using an improved resolution function and optimized coefficients  $f_k^i$ . For the latter, we include a dependence on  $\sigma_t$ , as this variable substantially improves the discrimination between signal decays and combinatorial background. We determine the  $\sigma_t$  distribution for combinatorial background by fitting WS data. To check the correctness of this method we generate MC samples with the same size as data, add the corresponding amount of backgrounds, and repeat the fitting procedure. For a wide range of  $(x'^2, y')$  values, the fit recovers the input values well within the statistical uncertainty. If the  $\sigma_t$  dependence is not included in  $f_k^i$ , the fit obtains values shifted by 0.5–1 statistical standard deviation with respect to the input values.

TABLE I: Summary of results including systematic errors.

| Fit case      | Parameter | Fit result   | 95% C.L. interval             |
|---------------|-----------|--|-------------------------------|
|               |           | ( $\times 10^{-3}$ )                                 | ( $\times 10^{-3}$ )          |
| No <i>CPV</i> | $R_D$     | $3.64 \pm 0.17$                                      | (3.3, 4.0)                    |
|               | $x'^2$    | $0.18^{+0.21}_{-0.23}$                               | $< 0.72$                      |
|               | $y'$      | $0.6^{+4.0}_{-3.9}$                                  | (-9.9, 6.8)                   |
|               | $R_M$     | -  | $(0.63 \times 10^{-5}, 0.40)$ |
| <i>CPV</i>    | $A_D$     | $23 \pm 47$  | (-76, 107)                    |
|               | $A_M$     | $670 \pm 1200$                                       | (-995, 1000)                  |
|               | $x'^2$    | -  | $< 0.72$                      |
|               | $y'$      | -  | (-28, 21)                     |
|               | $R_M$     | -  | $< 0.40$                      |
| No mixing     | $R_D$     | $3.77 \pm 0.08(\text{stat.}) \pm 0.05(\text{syst.})$ |                               |

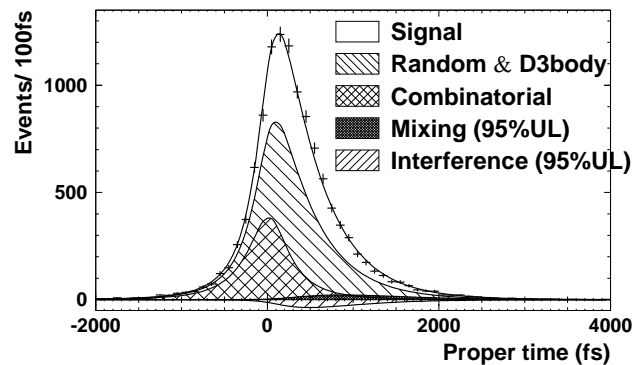


FIG. 2: The decay-time distribution for WS events satisfying  $|m_{K\pi} - m_{D^0}| < 22 \text{ MeV}/c^2$  and  $|Q - 5.9| < 1.5 \text{ MeV}$ . Superimposed on the data (points with error bars) are projections of the decay-time fit when no *CPV* is assumed. The mixing and interference terms are shown at the 95% confidence level upper limit (95% UL) for mixing.

Table I lists the results from three separate fits. For the

first fit, we require  $CP$  to be conserved. The projection of this fit superimposed on the data is shown in Fig. 2; the  $\chi^2$  of the projection is 54.6 for 60 bins. The central value of  $x'^2$  is in the physically-allowed region  $x'^2 > 0$ . The correlation between  $x'^2$  and  $y'$  is  $-0.909$ . The results for the two SVD subsamples are consistent within  $0.6\sigma$ . For the second fit, we allow  $CPV$  and fit the WS  $D^0$  and  $\bar{D}^0$  samples separately. We calculate  $A_D$  and  $A_M$  (see Table I), and solve for  $x'^2$ ,  $y'$  and  $\phi$  using Eqs. (2) and (3). We obtain  $|\phi| = (9.4 \pm 25.3)^\circ$  or  $(84.5 \pm 25.3)^\circ$  for the same or opposite signs of  $x'^+$  and  $x'^-$ . Finally, for the last fit we assume no mixing and set  $x'^2 = y' = 0$ .

We apply the method described in Ref. [6] to obtain the 95% confidence level (C.L.) region and take into account the systematic errors. Figure 3 shows the 95% C.L. contours with and without  $CPV$  allowed. For the case of no  $CPV$ , the allowed area of  $(x'^2, y')$  values is smaller than that of our previous measurement by a factor of 2.2. The  $CPV$  contour has a complicated shape due to there being two solutions for  $(x', y')$  when solving Eqs. (2) and (3), depending on the signs of  $x'^{\pm}$ .

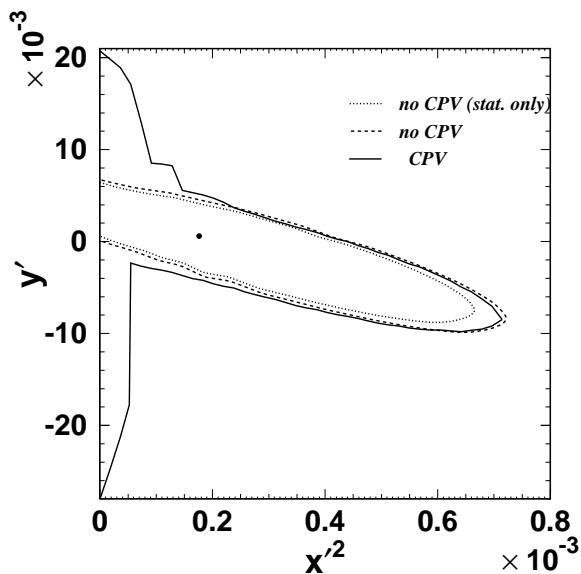


FIG. 3: 95% C.L. regions for  $(x'^2, y')$ . The point is the best fit result assuming  $CP$  conservation. The dotted (dashed) line is the statistical (statistical and systematic) contour for no  $CPV$ . The solid line is the statistical and systematic contour in the  $CPV$ -allowed case.

We evaluate systematic errors by varying parameters used to select and fit the data within their uncertainties. The sources of systematic error include event yields and imperfect modeling of backgrounds and uncertainties in the decay-time PDF's. The former were estimated by changing the selection criteria (kaon and pion identification,  $\chi^2$  of vertex fits, and the  $D^*$  momentum) and thus

the signal to background ratio over a significant range. The significance of an individual systematic shift is found by calculating  $m^2 = -2[\ln L(\vec{\alpha}_{\text{new}}) - \ln L(\vec{\alpha}_0)]/2.3$ , with  $\vec{\alpha}_{\text{new}} = (x'^2_{\text{new}}, y'_{\text{new}})$  denoting the result of the fit with the modified parameter and  $\vec{\alpha}_0$  the result from the default fit. The factor 2.3 corresponds to 68% confidence in two dimensions. The largest shift occurs for the  $D^*$  momentum selection; it is found to be  $m^2 = 0.083$ . The parameters of functions fitted to the  $m_{K\pi}$  and  $Q$  distributions were also varied by their corresponding uncertainties and the decay-time fit was repeated. The resulting systematic error is found to be small. The influence of  $\sigma_t$  on the fractions  $f_k^i$  is checked by obtaining the combinatorial background  $\sigma_t$  PDF from the fit to sideband events. Repeating the time fit with the modified  $f_k^i$  yields  $m^2 = 0.030$ . The same value is found when varying all of the fixed parameters entering the decay-time PDF's by their uncertainty. Adding in quadrature the significances of all shifts due to possible systematic uncertainties, we find the overall scaling factor  $\sqrt{1 + \sum m_i^2} = 1.12$ . We increase the 95% C.L. statistical contour by this factor to include systematic errors.

We show the contour with systematic errors included in Fig. 3 as a dashed line in the  $CP$ -conserving case and as a solid line in the general case. In the case of no  $CPV$ , the no-mixing point  $x'^2 = y' = 0$  lies just outside the 95% C.L. contour; this point corresponds to 3.9% C.L. with systematic uncertainty included. The two-dimensional 95% C.L. intervals of parameters listed in Table I are obtained by projecting these contours onto the corresponding coordinate axes. In the case of  $CPV$ , because the 95% C.L. contour includes the point  $x'^2 = y' = 0$ , we cannot constrain  $\phi$  at this confidence level.

In summary, we have searched for  $D^0$ - $\bar{D}^0$  mixing and  $CP$  violation in “wrong-sign”  $D^0 \rightarrow K^+\pi^-$  decays using a  $400 \text{ fb}^{-1}$  data sample. Assuming negligible  $CP$  violation in the  $D^0$  system, we obtain  $x'^2 < 0.72 \times 10^{-3}$  and  $-9.9 \times 10^{-3} < y' < 6.8 \times 10^{-3}$  at 95% C.L. These results supercede our previous measurement and represent the most stringent limits on  $D^0$ - $\bar{D}^0$  mixing parameters to date. The data exhibits a small preference for positive  $x'^2$  and  $y'$ ; the no-mixing point  $x'^2 = y' = 0$  corresponds to a C.L. of 3.9%.

We thank the KEKB group for excellent operation of the accelerator, the KEK cryogenics group for efficient solenoid operations, and the KEK computer group and the NII for valuable computing and Super-SINET network support. We acknowledge support from MEXT and JSPS (Japan); ARC and DEST (Australia); NSFC and KIP of CAS (contract No. 10575109 and IHEP-U-503, China); DST (India); the BK21 program of MOEHRD, and the CHEP SRC and BR (grant No. R01-2005-000-10089-0) programs of KOSEF (Korea); KBN (contract No. 2P03B 01324, Poland); MIST (Russia); MHEST (Slovenia); SNSF (Switzerland); NSC and MOE (Taiwan); and DOE (USA).

- 
- [1] G. Burdman and I. Shipsey, *Annu. Rev. Nucl. Part. Sci.* **53**, 431 (2003).
- [2] Charge-conjugate modes are included throughout this Letter unless noted otherwise.
- [3] E. Aitala *et al.* (E791 Collaboration), *Phys. Rev. D* **57**, 13 (1998).
- [4] R. Godang *et al.* (CLEO Collaboration), *Phys. Rev. Lett.* **84**, 5038 (2000).
- [5] B. Aubert *et al.* (BABAR Collaboration), *Phys. Rev. Lett.* **91**, 171801 (2003).
- [6] J. Li *et al.* (Belle Collaboration), *Phys. Rev. Lett.* **94**, 071801 (2005).
- [7] J. M. Link *et al.* (FOCUS Collaboration), *Phys. Lett. B* **618**, 23 (2005).
- [8] S. Kurokawa and E. Kikutani *et al.*, *Nucl. Instrum. Methods Phys. Res. Sect. A* **499**, 1 (2003).
- [9] A. Abashian *et al.* (Belle Collaboration), *Nucl. Instrum. Methods Phys. Res. Sect. A* **479**, 117 (2002).
- [10] Y. Ushiroda (Belle SVD2 group), *Nucl. Instrum. Methods Phys. Res. Sect. A* **511**, 6 (2003).
- [11] S. Eidelman *et al.* (Particle Data Group Collaboration), *Phys. Lett. B* **592**, 1 (2004).